Unexpected behavior of sodium sulfate observed in experimental freezing and corrosion studies

Ahmed Abdelmonem[1] | **Nikoleta Morelová[2]** | **Nicolas Finck[2]** |
Dieter Schild | **Johannes Lützenkirchen[2]**

[1]Institute of Meteorology and Climate Research   Atmospheric Aerosol Research (IMK AAF), Karlsruhe Institute of Technology (KIT), Eggenstein Leopoldshafen, Germany

[2]Institute for Nuclear Waste Disposal (INE), Karlsruhe Institute of Technology (KIT), Eggenstein Leopoldshafen, Germany

Correspondence
Ahmed Abdelmonem, Institute of Meteorology and Climate Research Atmospheric Aerosol Research (IMK AAF), Karlsruhe Institute of Technology (KIT), 76344 Eggenstein Leopoldshafen, Germany.
Email: ahmed.abdelmonem@kit.edu

Johannes Lützenkirchen, Institute for Nuclear Waste Disposal (INE), Karlsruhe Institute of Technology (KIT), Eggenstein Leopoldshafen, Germany
Email: johannes.luetzenkirchen@kit.edu

Abstract
This article reports results from two distinct, originally unrelated studies that show unexpected behavior with respect to sodium sulfate solutions in contact with flat surfaces. On the one hand, we investigated immersion freezing of sulfate containing solutions (target salt was $CaSO_4$ and Na_2SO_4 was used as one control) in the presence of flat sapphire-0001 crystals using second-harmonic generation (SHG) spectroscopy. Further control experiments were carried out with neat water and $CaCl_2$. The SHG signals from $CaSO_4$ and Na_2SO_4 solutions behave somewhat differently from those recorded for the two other cases, the neat water and $CaCl_2$. The common pattern shows a decrease of the SHG signal with decreasing temperature down to about $-15°C$, whereupon the signal sharply drops, indicating freezing. With the Na_2SO_4 solution, although the signal initially follows closely the neat water curve, the trend increases sharply at about $-10°C$ followed by a gradual decrease with further cooling. There is no plausible explanation for the distinct behavior of the Na_2SO_4 solution, and thermodynamic calculations do not suggest any precipitation of a sodium sulfate solid phase. At the end of the freeze–thaw cycle, the initial SHG for each system is retrieved, suggesting reversibility. On the other hand, in a separate investigation unrelated to the freezing study, it was repeatedly observed that sodium sulfate precipitates from solution on flat steel surfaces at room temperature. As in the freezing experiments, thermodynamic calculations for the bulk solution solubility of sodium sulfate indicate that precipitates should not be forming under the conditions of the studies. The crystals observed on the steel samples have snowflake shapes similar to one literature report. We conclude that Na_2SO_4 in the presence of flat surfaces shows unexpected behavior that should incite further detailed studies in the future to elucidate the phenomenon.

KEYWORDS
corrosion, immersion freezing, second harmonic generation, sodium sulfate

1 | INTRODUCTION

Atmospheric aerosols improve heterogeneous ice nucleation in the atmosphere through different freezing pathways (e.g., immersion mode that is the most important in mixed-phase clouds[1−3]). Immersion mode leads to the freezing of a supercooled cloud droplet or aqueous solution, in the presence of aerosol surface, at a temperature above approximately −38°C (the homogeneous freezing temperature).[4] The formation of ice in clouds has a significant influence on climate changes. Mineral dusts are considered as effective ice nuclei in the atmosphere.[4] Experimental freezing studies show a wide variability of the onset temperatures in terms of particle size,[5] surface properties,[6] and cloud droplet pH.[7] It has been demonstrated that ice nucleation is favored at microscopic, active sites.[8−11] In a previous study, on the 0001-cut α-Al$_2$O$_3$ surface, it was found that surface templating by induced charge may suppress nucleation.[12] Aerosol surface aging may also change the ice nucleation properties.[13] Chemical, structural, and physical properties of the ice nucleating particles account for the overall variability in nucleation properties.[14−16] Nonlinear optical (NLO) spectroscopic methods, mainly sum-frequency generation (SFG) and second-harmonic generation (SHG),[7] allow to elucidate the water structure at surfaces and interfaces on the molecular level. The signal strength and polarization configuration signpost the abundance and molecular structuring of the interfacial molecules, respectively.[17−20]

Ice nucleation studies showed that sulfuric-acid-coated atmospheric particles exhibit lower ice nucleation efficiency than those uncoated.[21,22] Yang et al[23] attributed this phenomenon to the degree of order of water molecules at the interface. They probed the water structure next to a mica surface, at room temperature, using SFG spectroscopy and realized that water ordering was drastically reduced in the presence of sulfuric acid. Here, we use SHG spectroscopy to compare the change in water structure upon immersion freezing of two sulfate containing solutions (CaSO$_4$ and Na$_2$SO$_4$) next to sapphire (α-alumina) which is an atmospherically relevant mineral oxide surface.[24−26] We measured the SHG signal as a function of temperature while cooling the sample from room temperature to the homogeneous freezing point. We kept all experimental conditions (concentrations of the divalent ions, solution volume, and temperature ramp) identical for all experiments to allow for direct comparison. We found that the effect of sulfate on water structuring next to the surface, and hence the ice nucleation ability of the surface, is not necessarily a depression of the ice nucleation efficiency, rather it may enhance the nucleation process.

Surprisingly, Na$_2$SO$_4$ enhanced the interfacial structure at the phase change temperature. Whether this was due to freezing and involved a significantly increased freezing temperature or whether a sodium sulfate solid precipitated is not clear from our preliminary measurements.

In a separate study, related to metallic corrosion which was initially disconnected from the freezing study, it was also noted that sodium sulfate showed some unexpected behavior. This corrosion study is related to nuclear waste disposal where the corrosion behavior of candidate materials for steel containers needs to be investigated and one testing solution used in the experiments contained Na$_2$SO$_4$. The safest and widely accepted choice for the final disposal of long-lived intermediate level (ILW) and high-level radioactive waste (HLW) are deep geological repositories. In these facilities, HLW is anticipated to be contained in thick-walled containers made of steel or copper. For example, the stainless steel 309S can be the primary package containing vitrified waste, whereas the ductile iron GGG40.3 may be one of the main materials used to construct containers for spent nuclear fuel. During the long-term evolution of such repositories, water will move through the barriers and reach the emplacement caverns leading to metallic corrosion. The objective of the corrosion experiments was to investigate the corrosion behavior of both selected materials under conditions corresponding to the aqueous systems in salt rock formations.[27,28] The major focus was the characterization of the formed secondary phases on the steel surface. In the present case, this also included the study of sodium sulfate containing solutions.

2 | EXPERIMENTAL

Materials and methods are explained in details in the supporting information. The chemicals (Na$_2$SO$_4$, CaCl$_2$, & CaSO$_4$) were obtained from VWR and used as received. The concentrations of the divalent ions in the solutions were kept constant at 15 mM. For consistency, the SHG data reported here were collected on the same single crystal sample, which was obtained from Victor Kyburz AG, Safnern, Switzerland. For the corrosion experiments, two steel types were obtained from ThyssenKrupp Acciai Speciali Terni (Stainless steel 309S) and Mittelrheinische Metallgießerei Heinrich Beyer GmbH (ductile iron GGG40.3) (Table S1 shows the chemical composition of the two specimens). The specimens were cut, polished, cleaned, and finally characterized by scanning electron microscopy (SEM), see supporting information and Figure S1.

To investigate the immersion freezing of CaSO$_4$ and Na$_2$SO$_4$ solutions next to the sapphire surface, a

homemade measuring cell was used in the SHG measurements. The prism-like sample was attached to an accurate cold-stage (Linkam model HFS-X350). A femtosecond laser system (Solstice, Spectra Physics) of 800-nm wavelength and 1-kHz pulse repetition rate was used to generate the SHG signal. More details on the experimental setup can be found in Abdelmonem et al[13] and is briefly repeated in the supporting information.

The corrosion experiments were carried out in tightly closed autoclaves. The steel coupons were placed onto a stand made of Teflon and fully submerged in the brine with 5 cm^3/cm^2 brine volume to surface area ratio. The brines used in the corrosion experiments (Table S2) were prepared according to literature that reports the Asse[29] and Gorleben[27] salt dome brine composition. The specimens were corroded in the autoclaves under anoxic conditions set in an argon-filled glove box for 182 days at room temperature. Following the exposure, the corroded coupons were rinsed with deionized water and blown dry before analysis by X-ray photoelectron spectroscopy (XPS), scanning electron microscopy (SEM), and energy dispersive X-ray spectroscopy (EDX). More details on the corrosion experiments are given in the supporting information.

Thermodynamic calculations were carried out using PhreeqC.[30] For the freezing study, the calculations involved the use of parameters for supercooled systems such as those published by Marion and Kargel[31] and Marion et al.[32] For the more concentrated solutions, the Pitzer model[33] with the appropriate parameters[34] was used to evaluate the potential formation of solid phases in the solutions used in the corrosion study.

3 RESULTS AND DISCUSSION

Figure 1 shows the SHG results from the freeze–thaw cycles for the various systems studied. The recorded SHG signal is plotted as a function of temperature. The blue lines are the cooling curves, whereas the red lines are the heating curves. The numbers indicate the sequence of the experiments. The addition of the different salt combinations to the measuring cell was done at room temperature. The concentration was 15 mM with respect to the divalent ion(s) present. Prior to testing a new system, the cell was thoroughly rinsed with MilliQ water, and the signal in the presence of neat water was checked. The order of the systems studied was H_2O, $CaCl_2$, Na_2SO_4, H_2O, and finally $CaSO_4$. The initial interest was in the $CaSO_4$ system, because the concentration range studied is not far from the solubility maximum. However, the run with the Na_2SO_4 system resulted in the most interesting outcome. This is also why we carried out a second water experiment after the Na_2SO_4 system to verify if properties of the crystal surface had changed.

Figure 1a–d shows the individual freeze–thaw cycles for the four systems. The results show that the freeze–thaw cycles were reversible in the sense that the SHG signal at the starting point at room temperature was always obtained again. The heating curves from the
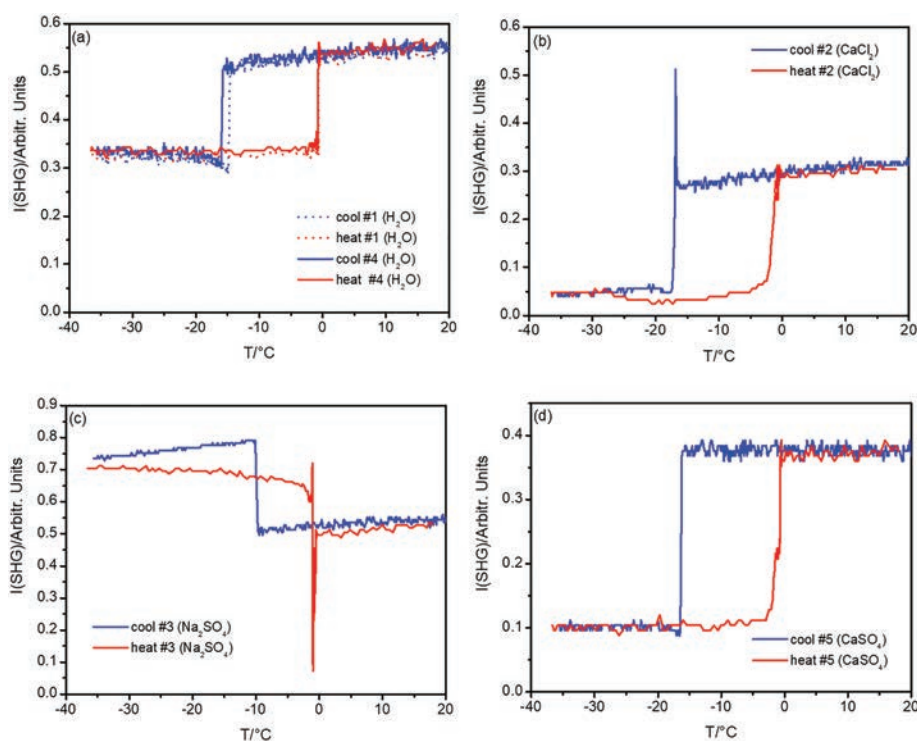
FIGURE 1 Freeze–thaw cycles for water (a) and 15 mM solutions of $CaCl_2$ (b), Na_2SO_4 (c), and $CaSO_4$ (d)

immersion freezing experiments show consistent melting close to 0°C. On the parts of the data, where both for cooling and heating liquid (at $T > 0°C$) or solid (at $T < T_{PC}$) were present, the data coincide for water and $CaSO_4$, and for $CaCl_2$ for the liquid. For the other cases, there is a clear hysteresis, which is not due to the phase changes or changes at the interface. The spikes in the SHG signal, clearly visible at the phase change in panels b and c, are the so called "transient signals." These arise from the fast changes in the refractive indices at the interface right after the phase change and have no chemical connotation. Origins of the transient signal have been explained elsewhere[13,35] and will not be further discussed here.

For water, $CaCl_2$, and Na_2SO_4, an initial decrease in water ordering with cooling takes place until the phase change occurs, whereas for $CaSO_4$, the signal initially remains constant with temperature, and then shows a transient signal before exhibiting the usual sharp drop that indicates phase change. For Na_2SO_4, the phase change clearly occurs at higher temperature than for the other systems, and the phase change in this case causes an increase in signal, while for the other solutions a decrease occurs. Further cooling causes the signal in the Na_2SO_4 system to clearly decrease, whereas in the other systems, it remains more or less constant.

The freezing curves are shown in summary in Figure 2a. Besides the clear exception in behavior of the Na_2SO_4 system, the comparison indicates that at room temperature, the Na_2SO_4 system behaves as water, which would indicate that there is no specific adsorption of sodium or sulfate under the given conditions in this case. The strongest drop with respect to water occurs in the $CaCl_2$ system suggesting that in this case, the Ca is probably most strongly interacting with the surface. Because Ca forms ion pairs in solution with sulfate, the slightly higher signal in the $CaSO_4$ system may be due to a decrease in free Ca concentration, but clearly sodium and sulfate ions do not seem to have any significant interaction with the surface relative to pure water. Figure 2b shows the corresponding heating curves. At the end of

each run, the signal before the start of the cooling ramp was retrieved.

In an extensive literature search, we did not find any hint for why the Na_2SO_4 system would behave in the way we observed. It is also not clear what was the cause for the sharp signal increase. However, in an earlier study, we have shown that adsorbed ions may form a network on the surface that alters its structure with concentration and is capable of enhancing the water structure and correspondingly the onset of the freezing next to the surface.[13] Thus, the sharp signal increase can be attributed to a well-structured ice forming much earlier than for the other systems or another phase change involving sodium sulfate. Although the solubility of Na_2SO_4 in aqueous solution is somewhat exceptional with a phase change at about 30°C,[36] there is no indication that a solid phase would form with the concentrations applied in the present study. Above about 30°C, the stable phase is thenardite, whereas below, it is mirabilite, also known as Glauber's salt. One additional phase is the metastable heptahydrate that has been reported to form in the presence of particles like quartz or calcite,[37,38] but even in these studies, solution concentrations are much higher than in the present case. However, there seems to be a clear trend with temperature as well in the above cited studies, with lower temperatures favoring the nucleation of the heptahydrate. We believe that the heptahydrate could be causing the strong increase in SHG in the Na_2SO_4 system. However, more work is required to understand this system. Another study in the absence of added particles appears to suggest that mirabilite is favored at lower temperatures.[39] Unfortunately, all these studies were carried out with solute concentrations at the higher end (i.e., above 1 M). Both our own speciation calculations and previous calculations reported in the literature[40,41] suggest that for bulk solutions with the solution concentrations involved, no solid should precipitate at the relevant temperature and that much higher equilibrium concentrations for sodium and sulfate are required for the solids to form. The presence of the surface may, however, catalyze the formation of precipitates.
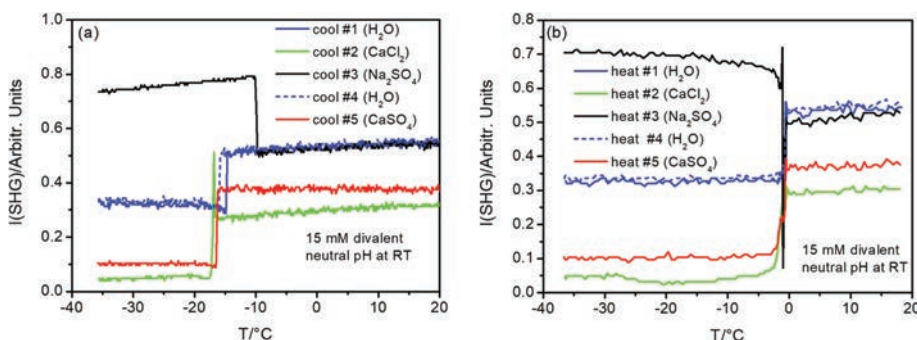
FIGURE 2   Comparison of the freezing (a) and heating (b) curves for all systems studied

This has been known for some time and has been modeled by the surface precipitation model[42–44] at room temperatures, and also directly observed.[45] The model covers in principle the transition from adsorption to solid solution formation (complete mixing between the surface-constituting mineral[42]) and to heterogeneous nucleation (resulting in a BET-type[46] isotherm equation[44]). The resulting "interfacial" solubility products in such modeling studies were significantly lower compared with the respective values in bulk solution for otherwise identical conditions. It has been argued that electrostatic fields at the interface might be one reason for this lowered solubility.[44] In the present case, two orders of magnitude difference between the inferred solubility in the presence of the surface and the calculated solubility in its absence[41] is within the range of published differences for other systems. However, it is clear that the mechanism leading to the observed SHG results will need to be studied separately for understanding the process.

In the corrosion studies, which are discussed in the following, the sulfate concentrations were higher than in the freezing studies. The optical microscopy images of the post-corrosion steel specimens (Figure 3) show the presence of various precipitates. For the stainless steel, the effect appears to be more significant for the specimen in Solution 1 (the composition of Solutions 1 and 3 are given in Table S2, Solution 1 contains 310 mM NaCl and 150 mM sulfate, while Solution 3 contains 5 M NaCl and 34 mM sulfate), whereas for the ductile iron, the precipitates appear to be similar for both solutions. The postmortem XPS analyses of the surface showed the presence of Cr(III), Ni(0), and Fe(0) for the stainless steel samples, matching the surface analyses prior to the start of corrosion experiments and highlighting lack of corrosion products other than an intact protective Cr_2O_3 layer. More interestingly, in both cases, XPS S 2p spectra showed the presence of sulfate on the studied surfaces. This corresponds to the regions of the visible precipitates in Figure 3 (spectrum for stainless steel sample in Solution 1 shown in Figure 4a). Similarly, for the ductile iron samples, the postmortem XPS analyses showed the presence of sulfate in S 2p spectra for both solutions. The spectrum for ductile iron sample in Solution 1 is shown in Figure 4b.

SEM revealed for all samples precipitates with snowflake-like morphology (Figures 5 and 6). The EDX analyses of these precipitates pointed to sodium sulfate, with the chemical composition of Na: 30–33 at. %, S: 15–17 at. %, O: 49–51 at. % and trace amounts of Fe and Cr originating from the steel and K, Cl, and Mg originating from the solutions. Rodriguez-Navarro et al[47] also describe the crystallization of sodium sulfate in the form with the morphology observed in this work. Sodium sulfate is a distinct component of Solution 3, whereas in Solution 1, the salt components are NaCl and $MgSO_4$, but in both cases, the amounts are below the saturation limit as was verified by PhreeqC calculations. Such simple generic calculations with PhreeqC, however, do not take into account the reactive surface, whereas a more complex model accounting for the surface and reaction conditions may provide different results and explain the precipitation of sodium sulfate. To our knowledge,

FIGURE 3 The specimens after corrosion. (a) Stainless steel in Solution 3, (b) stainless steel in Solution 1, (c) ductile iron in Solution 3, (d) ductile iron in Solution 1
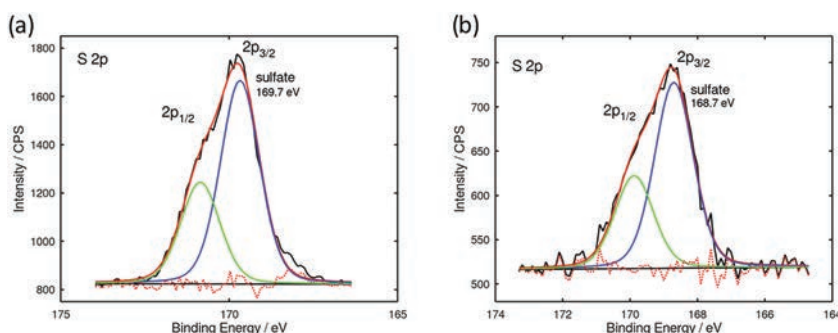
FIGURE 4 The X ray photoelectron spectroscopy (XPS) S 2p spectrum for (a) stainless steel sample in Solution 1 and (b) ductile iron sample in Solution 1
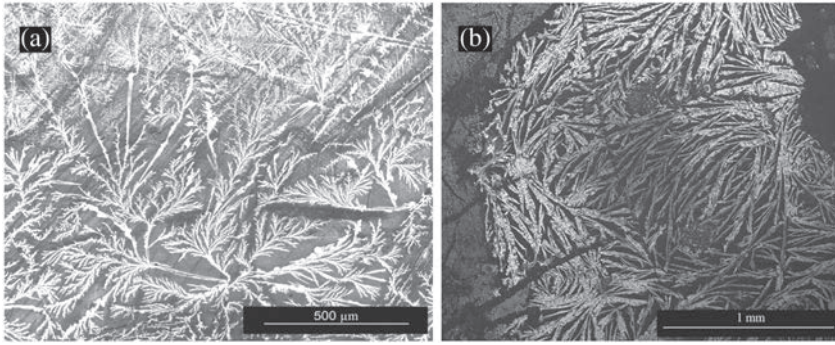
FIGURE 5 Scanning electron micrographs of the stainless steel corroded in Solutions 3 (a) and 1 (b)
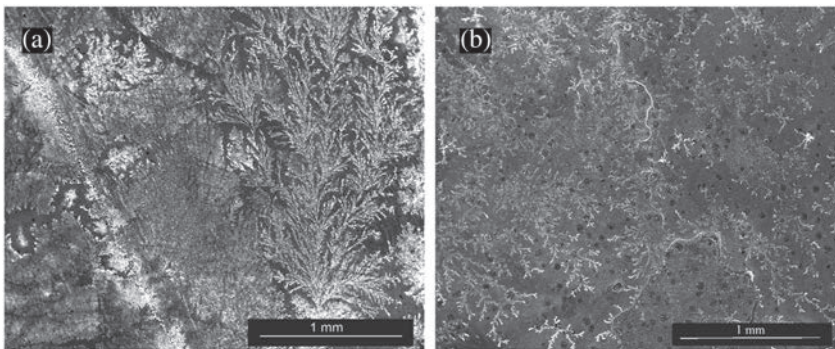
FIGURE 6 Scanning electron micrographs of the ductile iron corroded in Solutions 3 (a) and 1 (b)

currently no such model exists, and therefore, the bulk solubility calculations are the only way to relate the observation to thermodynamic data. The reason for the precipitation of this compound is not yet clear. This observation was repeatedly made in four distinct samples, in four different autoclaves, and with two steel types and various brines. Thus, the occurrence of the same artifact in samples with various surfaces (stainless steel and ductile iron) is unlikely. However, the exposure was only for 182 days, and the experiments were not repeated for longer exposure. To verify if the observed solid phase is stable, more experimental work will be required, and longer equilibration times should be part of such work. As for the SHG study, it is also possible that the surface precipitation is favoring the formation of the solid even under conditions where it would not form in the absence of the solid.[42–45]

4 CONCLUSIONS

In two types of experiments from separate disciplines, unexpected behavior of sodium sulfate containing solutions was observed. In the SHG freezing study down to −10°C, the sodium sulfate solution behaved very much like water, which suggests no particular interaction of the ions with the surface. Other solutions clearly showed interaction e.g. in Ca-containing systems to occur at room temperature. At about −10°C, an early freezing and a distinctly different pattern in the freezing curve of sodium sulfate occurred with a sharp increase in the SHG signal followed by a continuous decrease. At the temperature of phase change in the sodium sulfate system, the signal increased while it decreased in all other systems. We suggest this is most likely due to the formation of a solid sodium sulfate phase. This interpretation would be corroborated by the independent corrosion study. In the corrosion experiments, similarly unexpected, the presence of sodium sulfate was observed on surfaces under conditions for which this compound is below saturation based on thermodynamic calculations for bulk solutions. In the corrosion study, the crystals were imaged and identified. The shape of the formed crystals compared well with those previously reported in a cement-related study.[47] There is currently no clear explanation for the observations. The reported results are empirical in the sense that we have observed an unexpected phenomenon in the presence of sodium sulfate solutions in two initially unrelated studies. Previous observations and model calculations suggest that the presence of a surface can catalyze the formation of surface precipitates under conditions where the precipitates would not form in the bulk of the solution (i.e., in the absence of a surface).[42–45] Currently, we have no direct explanation for our observations, and more work will be required to provide deeper insights.

ORCID

Ahmed Abdelmonem https://orcid.org/0000-0002-4348-2439

Nikoleta Morelová https://orcid.org/0000-0002-7448-9107

Nicolas Finck https://orcid.org/0000-0002-1940-4051

Dieter Schild https://orcid.org/0000-0001-6034-8146

Johannes Lützenkirchen https://orcid.org/0000-0002-0611-2746

REFERENCES

[1] A. Ansmann, M. Tesche, D. Althausen, D. Müller, P. Seifert, V. Freudenthaler, B. Heese, M. Wiegner, G. Pisani, P. Knippertz, O. Dubovik, *J. Geophys. Res.: Atmos.* **2008**, *113*(D4), D04210.

[2] G. de Boer, H. Morrison, M. D. Shupe, R. Hildner, *Geophys. Res. Lett.* **2011**, *38*, L01803. http://dx.doi.org/10.1029/2010gl046016

[3] C. D. Westbrook, A. J. Illingworth, *Q. J. Roy. Meteorol. Soc.* **2013**, *139*(677), 2209.

[4] H. R. Pruppacher, J. D. Klett, *Microphysics of Clouds and Precipitation*, 2nd ed., Kluwer Academic Publishers, Dordrecht, Boston **1997** 954.

[5] C. Hoose, O. Mohler, *Atmos. Chem. Phys.* **2012**, *12*(20), 9817.

[6] G. Kulkarni, S. Dobbie, *Atmos. Chem. Phys.* **2010**, *10*(1), 95.

[7] Y. R. Shen, *Nature* **1989**, *337*(6207), 519.

[8] G. W. Bryant, J. Hallett, B. J. Mason, *J. Phys. Chem. Solid* **1960**, *12*(2), 189.

[9] M. L. Corrin, J. A. Nelson, *J. Phys. Chem.* **1968**, *72*(2), 643.

[10] A. C. Zettlemoyer, N. Tcheurekdjian, C. L. Hosler, *Z. Angew. Math. Phys.* **1963**, *14*(5), 496.

[11] A. Kiselev, F. Bachmann, P. Pedevilla, S. J. Cox, A. Michaelides, D. Gerthsen, T. Leisner, *Science* **2017**, *355*(6323), 367. https://doi.org/10.1126/science.aai8034

[12] A. Abdelmonem, E. H. G. Backus, N. Hoffmann, M. A. Sánchez, J. D. Cyran, A. Kiselev, M. Bonn, *Atmos. Chem. Phys.* **2017**, *17*(12), 7827.

[13] A. Abdelmonem, S. Ratnayake, J. D. Toner, J. Lützenkirchen, *Atmos. Chem. Phys.* **2020**, *20*(2), 1075.

[14] E. Anim Danso, Y. Zhang, A. Alizadeh, A. Dhinojwala, *J. Am. Chem. Soc.* **2013**, *135*(7), 2734.

[15] P. Conrad, G. E. Ewing, R. L. Karlinsey, V. Sadtchenko, *J. Chem. Phys.* **2005**, *122*(6), 064709. 1 064709 11

[16] X. L. Hu, A. Michaelides, *Surf. Sci.* **2007**, *601*(23), 5378.

[17] A. Abdelmonem Nonlinear optical spectroscopy at the Liquid /Solid interface. Dissertation, Ruprecht – Karls – Universität, Heidelberg, **2008**.

[18] J. H. Jang, F. Lydiatt, R. Lindsay, S. Baldelli, *J. Phys. Chem. A* **2013**, *117*(29), 6288.

[19] Y. Rao, Y. S. Tao, H. F. Wang, *J. Chem. Phys.* **2003**, *119*(10), 5226.

[20] X. Zhuang, P. B. Miranda, D. Kim, Y. R. Shen, *Phys. Rev. B* **1999**, *59*(19), 12632.

[21] D. J. Cziczo, K. D. Froyd, S. J. Gallavardin, O. Moehler, S. Benz, H. Saathoff, D. M. Murphy, *Environ. Res. Lett.* **2009**, *4*(4), 044013.

[22] M. L. Eastwood, S. Cremel, M. Wheeler, B. J. Murray, E. Girard, A. K. Bertram, *Geophys. Res. Lett.* **2009**, *36*(2), L02811.

[23] Z. Yang, A. K. Bertram, K. C. Chou, *J. Phys. Chem. Lett.* **2011**, *2*(11), 1232.

[24] Z. A. Kanji, J. P. D. Abbatt, *J. Geophys. Res. Atmos.* **2006**, *111*(D16), D1620401.

[25] H. A. Al Abadleh, V. H. Grassian, *Langmuir* **2003**, *19*(2), 341.

[26] D. E. Brownlee, F. Horz, D. A. Tomandl, P. W. Hodge, *International Astronomical Union Colloquium* **1976**, *25*(2), 962.

[27] B. Kursten; E. Smailos; I. Azkarate; L. Werme; N. R. Smart; G. Santarini, COBECOMA. State of the art document on the Corrosion Behaviour of Container Materials. European Commission, contract no. FIKW CT 20014 20138, Final report. **2004**.

[28] F. King Corrosion of carbon steel under anaerobic conditions in a repository for SF and HLW in Opalinus Clay. NAGRA Technical report 08 12; Switzerland, **2008**; p 56.

[29] B. Kienzler; A. Loida Endlagerrelevante Eigenschaften von hochradioaktiven Abfallprodukten. Charakterisierung und Bewertung. Empfehlung des Arbeitskreises HAW Produkte. Wissenschaftliche Berichte FZKA 6651, Forschungszentrum Karlsruhe, **2001**. DOI: 10.5445/IR/270050533

[30] D. L. Parkhurst, C. Appelo, Description of input and examples for PHREEQC version 3: a computer program for speciation, batch reaction, one dimensional transport, and inverse geochemical calculations 2328–7055; US Geological Survey, **2013**.

[31] G. M. Marion, J. S. Kargel, *Cold Aqueous Planetary Geochemistry with FREZCHEM: From Modeling to the Search for Life at the Limits*, Springer, Berlin Heidelberg **2007**.

[32] G. Marion, D. Catling, K. Zahnle, M. Claire, *Icarus* **2010**, *207*(2), 675.

[33] K. S. Pitzer, *J. Phys. Chem.* **1973**, *77*(2), 268.

[34] C. E. Harvie, N. Moller, J. H. Weare, *Geochim. Cosmochim. Acta* **1984**, *48*(4), 723.

[35] A. Abdelmonem, E. H. G. Backus, M. Bonn, *J. Phys. Chem. C* **2018**, *122*, 24760.

[36] P. Bharmoria, P. S. Gehlot, H. Gupta, A. Kumar, *J. Phys. Chem. B* **2014**, *118*(44), 12734.

[37] H. Derluyn, T. A. Saidov, R. M. Espinosa Marzal, L. Pel, G. W. Scherer, *J. Cryst. Growth* **2011**, *329*(1), 44.

[38] T. A. Saidov, R. M. Espinosa Marzal, L. Pel, G. W. Scherer, *J. Cryst. Growth* **2012**, *338*(1), 166.

[39] C. Balarew, S. Tepavitcharova, S. Kamburov, *Monatshefte für Chemie Chemical Monthly* **2018**, *149*(2), 289.

[40] R. J. Spencer, N. Møller, J. H. Weare, *Geochim. Cosmochim. Acta* **1990**, *54*(3), 575.

[41] J. D. Toner, D. C. Catling, *J. Chem. Eng. Data* **2017**, *62*(10), 3151.

[42] K. J. Farley, D. A. Dzombak, F. M. Morel, *J. Colloid Interface Sci.* **1985**, *106*(1), 226.

[43] R. N. Comans, J. J. Middelburg, *Geochim. Cosmochim. Acta* **1987**, *51*(9), 2587.

[44] J. Lützenkirchen, P. Behra, *Aquat. Geochem.* **1995**, *1*(4), 375.

[45] S. E. Fendorf, D. L. Sparks, M. Fendorf, R. Gronsky, *J. Colloid Interface Sci.* **1992**, *148*(1), 295.

[46] S. Brunauer, P. H. Emmett, E. Teller, *J. Am. Chem. Soc.* **1938**, *60*(2), 309.

[47] C. Rodriguez Navarro, E. Doehne, E. Sebastian, *Cem. Concr. Res.* **2000**, *30*(10), 1527.

Repository KITopen

Dies ist ein Postprint/begutachtetes Manuskript.

Empfohlene Zitierung:

Zitierung der Originalveröffentlichung: